Heliyon 10 (2024) e27023

Contents lists available at ScienceDirect

Heliyon

journal homepage: www.cell.com/heliyon

Research article

Identification and prognostic evaluation of differentially expressed long noncoding RNAs associated with immune infiltration in osteosarcoma

Bangmin Wang [a], Xin Wang [a], Xinhui Du [a], Shilei Gao [a], Bo Liang [b,*], Weitao Yao [a,**]

[a] Department of Bone Oncology, The Affiliated Cancer Hospital of Zhengzhou University & Henan Cancer Hospital, Zhengzhou, China
[b] Department of Nephrology, The Key Laboratory for the Prevention and Treatment of Chronic Kidney Disease of Chongqing, Chongqing Clinical Research Center of Kidney and Urology Diseases, Xinqiao Hospital, Army Medical University (Third Military Medical University), Chongqing, China

ARTICLE INFO

Keywords:
Osteosarcoma
Prognosis
lncRNA
Immune infiltration

ABSTRACT

Osteosarcoma is a malignant bone cancer that originates from the bone with the strongest invasiveness. Tumor formation strongly correlates with immune cell infiltration into the tumor immune microenvironment (TIME). Therefore, we aimed to identify TIME-related biomarkers as potential prognostic markers of osteosarcoma. The mRNA and long noncoding RNA (lncRNA) transcriptome data of 88 patients with osteosarcoma and the expression profile of GSE99671 were downloaded from The Cancer Genome Atlas and Gene Expression Omnibus, respectively. Immune infiltration scores and types were evaluated using ESTIMATE and CIBERSORT. A linear model was established to identify the differentially expressed genes (DEGs) and lncRNAs (DElncRNAs). Functional enrichment analysis of DEGs was conducted by Gene Ontology, Kyoto Encyclopedia of Genes and Genomes, gene set enrichment analysis, and gene set variation analysis. DElncRNAs were analyzed using a weighted gene co-expression network. Least absolute shrinkage and selection operator regression was applied to screen for prognostic markers. Patient survival was predicted by the risk score and analyzed by receiver operating characteristic curve. Clinical features affecting patient survival were assessed. Immune infiltration positively correlated with osteosarcoma patient survival. Different immune cell infiltrates in patients with osteosarcma may serve as prognostic indicators and targets for immunotherapy. In total, 1125 DEGs, 80 DElncRNAs, and 11 pairs of co-expressed lncRNA-mRNAs were identified. DEGs in the three modules were associated with immune infiltration into the TIME. Four DElncRNAs, namely AC015819.1, AC015911.3, AL365361.1, and USP30-AS1, showed good prognostic ability for osteosarcoma and were positively correlated with the immune score. Tumor metastasis and risk scores alone were good prognostic indicators, and a combination of the two variables can better predict the prognosis of osteosarcoma. We identified four lncRNAs, AC015819.1, AC015911.3, AL365361.1, and USP30-AS1, as potential biomarkers for osteosarcoma prognosis.

* Corresponding author.
** Corresponding author.
E-mail addresses: liangbo2018@126.com (B. Liang), zlyyyaoweitao1402@zzu.edu.cn (W. Yao).

https://doi.org/10.1016/j.heliyon.2024.e27023
Received 9 December 2023; Received in revised form 20 January 2024; Accepted 22 February 2024
Available online 28 February 2024

1. Introduction

Osteosarcoma is one of the most prevalent malignant bone cancers affecting children and adolescents [1]. Osteosarcoma incidence in different age groups shows bimodal changes, with the first peak occurring in children and adolescents, and the second peak occurring after 60 years of age [2]. Osteosarcoma is usually caused by the inability of osteoblasts to differentiate into mature osteoblasts, and its typical pathological manifestations include spindle cells and osteoid formation [3,4]. Further, osteosarcomas exhibit a high degree of local invasion and early metastasis [5]. Patients with osteosarcoma are at higher risk of developing a second malignancy [6]. Osteosarcoma treatment typically involves a combination of chemotherapy and surgical resection [7,8]. Nevertheless, survival has stagnated in recent years and the prognosis of patients with metastatic or recurrent osteosarcoma remains unsatisfactory, with a 5-year overall survival rate of 20% [2,9]. Therefore, an urgent need exists to understand the exact mechanism of osteosarcoma and identify potential prognostic biomarkers and new treatment targets to improve survival rates.

The tumor immune microenvironment (TIME) comprises endothelial and mesenchymal cells, extracellular matrix molecules, tumor-infiltrating immune cells, and inflammatory mediators [10]. TIME is involved in the occurrence, metastasis, and prognosis of tumors [11–13]. In the TIME, tumor-infiltrating immune cells constitute the main non-tumor component, which is valuable for the prognostic evaluation of osteosarcoma [14]. As reported, osteosarcoma patients with a higher content of immune cells in the TIME have a better prognosis [15]. Therefore, systematically evaluating the immune characteristics of the TIME, determining the distribution and function of tumor-infiltrating immune cells, and improving the immunotherapeutic effect on osteosarcoma are crucial.

Long noncoding RNAs (lncRNAs) are RNA molecules with more than 200 nucleotides that do not encode proteins [16]. LncRNAs, which account for approximately 80% of the human transcriptome, play an important regulatory role in various cancers by interacting with DNA, RNA, and proteins [17]. Moreover, lncRNAs are involved in various biological processes such as proliferation, apoptosis, and invasion of tumor cells [18]. Specifically, immune-associated lncRNAs influence the prognosis of osteosarcoma and are correlated with the TIME [15]. These lncRNAs regulate the TIME by regulating immune-related gene expression and disturbing immune cell infiltration into the TIME [19]. Therefore, lncRNAs play key roles in the pathogenesis of osteosarcoma.

Integrated bioinformatics analysis of microarray data is beneficial for uncovering functions and signaling processes associated with various physiological and pathological conditions [20]. Recent studies have identified osteosarcoma signaling pathways through bioinformatics analysis based on the Gene Expression Omnibus (GEO) database, providing potential diagnostic biomarkers for osteosarcoma, including serum miRNA panels [21,22]. However, public databases with extensive genomic profiling data from patients with osteosarcoma have not been thoroughly analyzed. Additionally, studies on the discovery of abnormal lncRNA expression in osteosarcoma through comprehensive bioinformatic analyses have not been reported. Therefore, this study sought to identify potential TIME-related biomarkers of osteosarcoma through bioinformatics analyses.

2. Materials and methods

2.1. Data extraction and preprocessing

The transcriptome data (mRNA and lncRNA) from sarcoma tissues of 88 osteosarcoma patients in the TARGET project were downloaded from The Cancer Genome Atlas (TCGA). Additionally, clinical characteristics and follow-up outcomes of the patients were obtained. The original count matrix and annotation files of the RNA sequencing results from transcriptome dataset GSE99671, containing osteosarcoma and normal bone tissues from reliable samples, were downloaded from GEO [23]. GSE99671 includes the mRNA transcriptome data of 18 osteosarcomas and 18 normal bone tissues.

2.2. Analysis of immune infiltration score

The ESTIMATE algorithm was employed to calculate the infiltration score of immune cells in tissues using transcriptome data. Specifically, we used the *Estimate* package (version 1.0.13) to calculate and compare the immune cell infiltration score based on osteosarcoma mRNA data from TCGA database across different clinical subgroups [24]. We applied the *Maxstat* package (version 0.7–2.5) and Cox regression to determine the cutoff value for immune scores. Subsequently, osteosarcoma patients were categorized into high and low expression groups of immune invasion based on the established cutoff value for further downstream analyses [25].

2.3. Analysis of immune cell infiltration

We used the gene expression matrix to compute the immune cell infiltration of samples using the CIBERSORTx online analysis tool, and samples wit significance level of $P < 0.05$ were retained for further analysis [26]. Differences in the degree of immune cell infiltration between the high and low immune score groups were analyzed using the Wilcoxon test. In instances where immune cells exhibited significant differences, we conducted a correlation analysis to evaluate the degree of infiltration among various immune cells.

2.4. Analysis of immune-related differentially expressed mRNAs/lncRNAs

The *limma* package (version 3.58.1) was used to evaluate differentially expressed genes (DEGs) and lncRNAs (DElncRNAs) in the high and low immune infiltration groups, employing a linear model [27]. The screening criteria for DEGs/DElncRNAs were set at $P <$

0.05 and $|\log_2 FC| > 1$. We employed the *ggplot2* package (version 3.4.4) to generate a volcanic map of DEGs/DElncRNA to present the outcomes of differential expression analysis. Furthermore, a Wayne diagram was constructed to illustrate the immune-related DEGs obtained from TCGA and GEO datasets [28].

2.5. Co-expression analysis of DEGs and DElncRNAs

We conducted co-expression analysis of immune-related DEGs and DElncRNAs, and calculated the Pearson correlation coefficient (PCC) between lncRNAs and mRNAs. Subsequently, we selected the lncRNA-mRNA pairs with an absolute PCC value ≥ 0.9 and $P < 0.05$ to construct the lncRNA-mRNA co-expression network. This network was then visualized by importing it into the regulatory network visualization software, Cytoscape (version 3.10.1) [29].

2.6. Functional enrichment analyses

Gene Ontology (GO) and Kyoto Encyclopedia of Genes and Genomes (KEGG) enrichment analyses were performed on DEGs following established protocols [30–32]. Gene set enrichment analysis (GSEA) and gene set variation analysis (GSVA) were also performed [33]. Finally, differential pathways were screened using the *limma* package, with a significance threshold set at $P < 0.05$ for screening.

2.7. Weighted gene co-expression network analysis (WGCNA)

The identified DElncRNAs were assessed using WGCNA. The DElncRNAs were analyzed for calculating the PCC of each lncRNA-mRNA pair using the *WGCNA* package (version 1.72–5) [34]. All the selected lncRNAs were annotated using LNCipedia (version 5.2) [35].

2.8. Least absolute shrinkage and selection operator (LASSO) analysis

Following the identification of immune-related DElncRNAs, univariate Cox regression was used to screen lncRNAs significantly associated with the survival of patients with osteosarcoma. Subsequently, LASSO regression analysis was used to further screen for prognostic markers [36]. The *glmnet* package (version 4.1–7) facilitated the screening process, considering combinations of diagnostic markers with a minimum coefficient of variation [37].

2.9. Risk score (RS) and prognosis prediction model construction

The formula for calculating the RS of each case was $RS = \sum_{i=1}^{n} Coef_i \times Exp_i$, where Coef represents the regression coefficient obtained from LASSO analysis, and Exp is the expression level of corresponding lncRNA (log2 converted). We used the *Maxstat* package (version 0.7–25) to determine the optimal cutoff value of RS for predicting osteosarcoma survival rate. Subsequently, patients with osteosarcoma were assigned to high and low-risk groups, and the survival curve was generated using the Kaplan-Meier method. We also predicted the survival time (1, 3, and 5 years) of patients using *survivalROC* package (version 1.0.3.1), plotted the predicted receiver operating characteristic (ROC) and calculated the area under the curve (AUC) value [38]. We used the Cox proportional hazard model to evaluate the impact of other clinical features (age, sex, and metastasis) on prognostic survival and the *forestmodel* package (version 0.6.2) to generate a forest plot [39]. Next, the clinical features that had significant effects on prognosis were incorporated into multivariate Cox regression analysis to evaluate the independent predictive ability of RS. Finally, we employed the *rms* package (version 6.7–1) to generate the nomograms and calibration curves for visualizing the multivariate model. Additionally, the consistency index (C-index) was calculated to evaluate the survival prediction ability of the nomogram.

2.10. Experimental validation

2.10.1. Cell culture and transfection

Human osteosarcoma cells (143 B, MG63, and SW1353) and human osteoblasts (hFOB 1.19) were obtained from the National Collection of Authenticated Cell Cultures (Shanghai, China) and cultured in specific media. Cells were cultured at 37 °C in a 5% CO_2 atmosphere for all experiments. Small-interfering RNA (siRNA) and a negative control (siCON) were synthesized by YouBio (Hunan, China). Lipofectamine™ 3000 (Thermo Fisher Scientific, Waltham, MA, USA) was used for cell transfection [40]. The target sequences for transient silencing are listed in Table S1.

2.10.2. Cell viability and apoptosis

Cell viability was assessed using a Cell Counting Kit-8 (CCK-8; Solarbio, Beijing, China) [41]. Apoptotic cells were assessed using the Annexin V-FITC/PI Apoptosis Detection Kit (Vazyme, Nanjing, China) [42].

2.10.3. Enzyme-linked immunosorbent assay (ELISA)

Cell supernatants were harvested and the level of TNF-α was determined by an ELISA kit (ELK1190, ELK Biotechnology, Wuhan,

China) as described previously [43].

2.10.4. Quantitative real-time polymerase chain reaction (qRT-PCR)

Total RNA was extracted with TRIzol Reagent (Vazyme). Subsequently, the extracted RNA was reverse-transcribed into cDNA using the cDNA Synthesis Kit (Yeasen, Shanghai, China), and quantified with Universal SYBR Green qPCR Supermix (UElandy, Suzhou, China), sequentially [44]. The primers utilized for these procedures were synthesized by Generay (Shanghai, China) and are listed in Table S2.

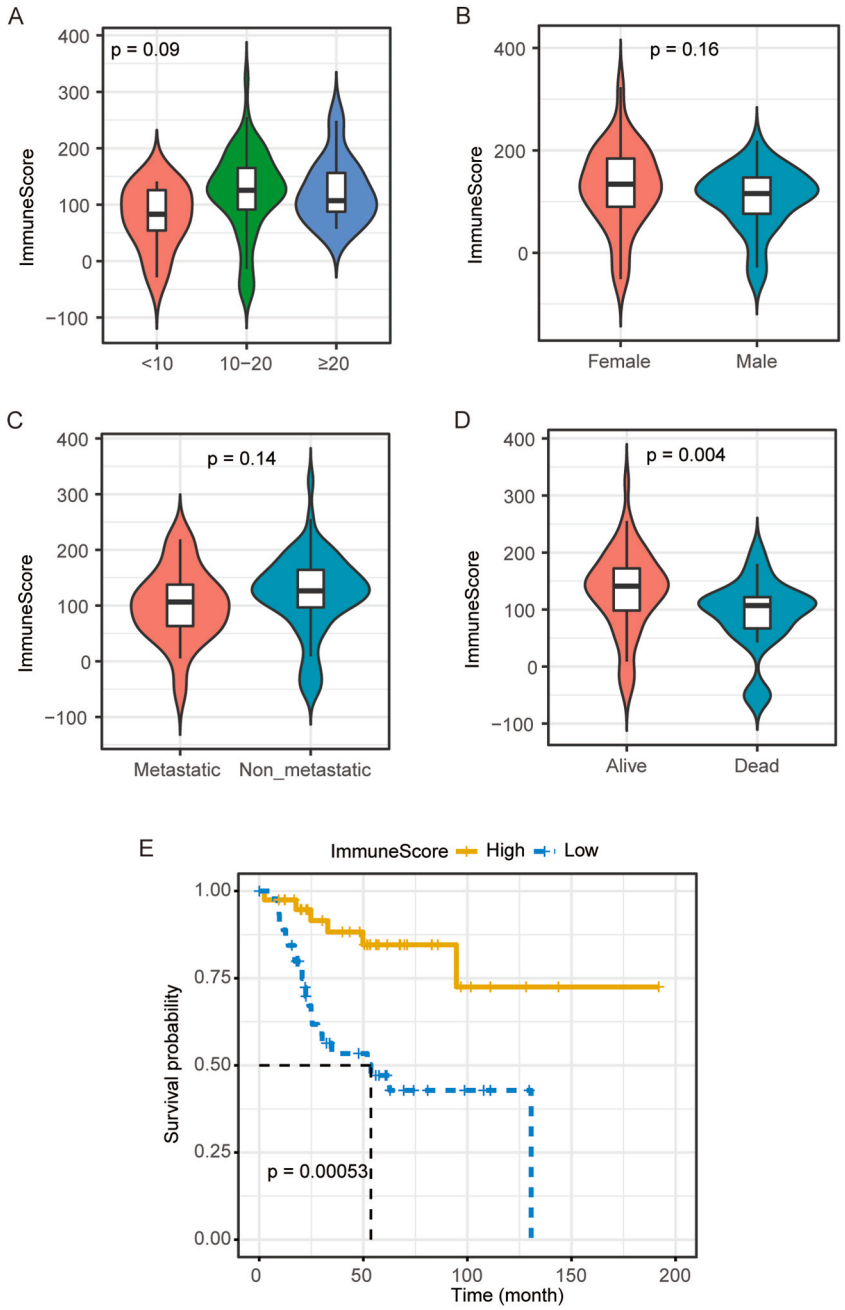

Fig. 1. Comparison of immune infiltration score in different clinical subgroups and its relationship with prognosis. A–C: Comparison of immune infiltration scores among the patients of different ages, sex, and metastasis; D: Comparison of immune infiltration scores between the survival and death groups; E: The K-M survival curve of the high/low immune score groups and prognosis.

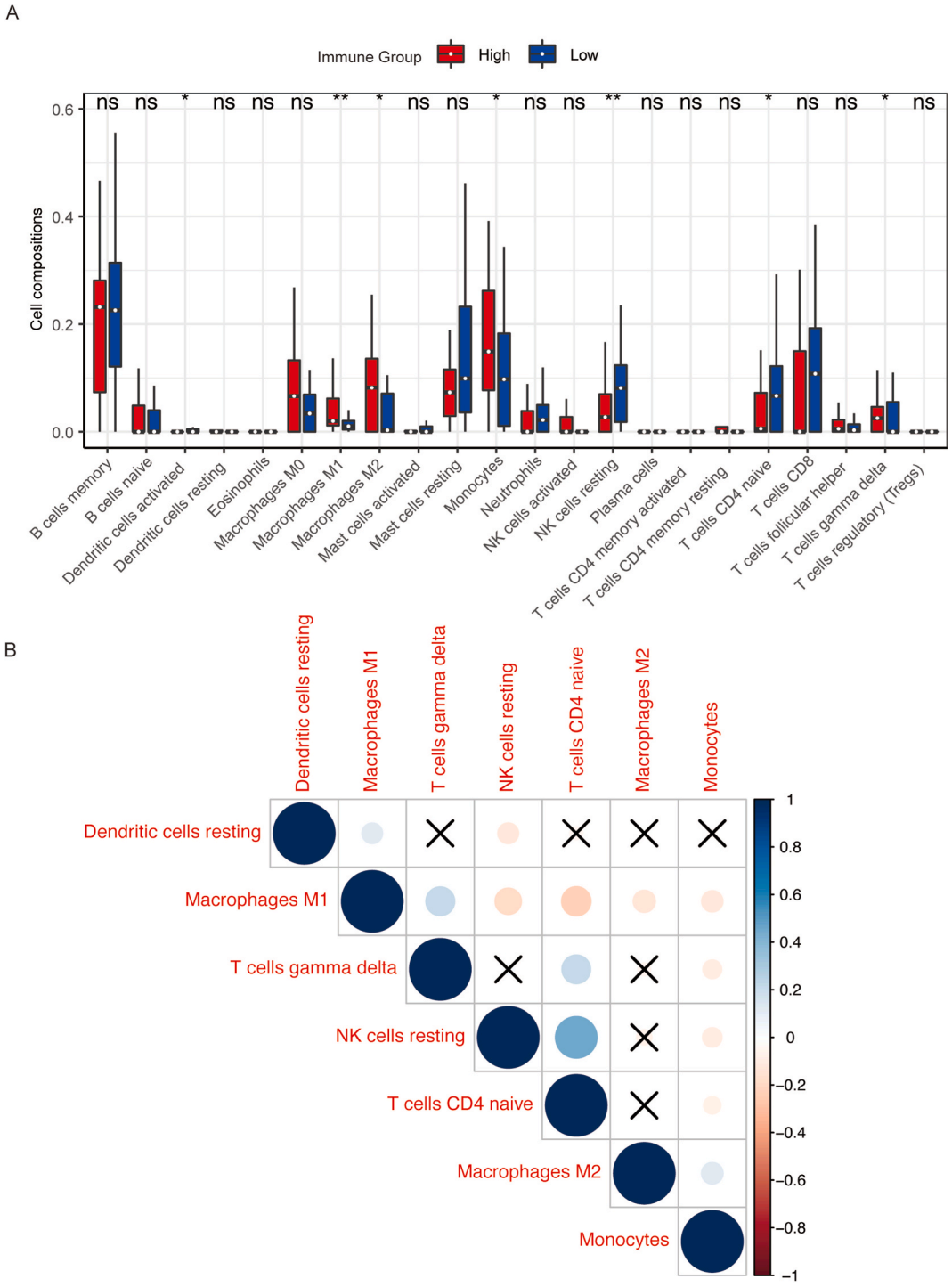

Fig. 2. Analysis of immune cell infiltration. A: Comparison of infiltration levels of different immune cells in the high/low immune score groups. Kruskal–Wallis test was used for comparisons between groups, and "*" indicated statistically significant differences. B: Correlation matrix between immune cells with the significant difference in the degree of infiltration in the high/low immune score groups; red represents positive correlation, blue represents negative correlation (darkness of the color reflects the degree of correlation), and the cells without statistical significance are represented by black X. (For interpretation of the references to color in this figure legend, the reader is referred to the Web version of this article.)

2.10.5. Transwell assay

Transwell migration assays were conducted to measure cell invasion as previously described [40].

2.11. Statistical analysis

All data calculations and statistical analyses were performed using the R software. The Benjamini-Hochberg test was used for

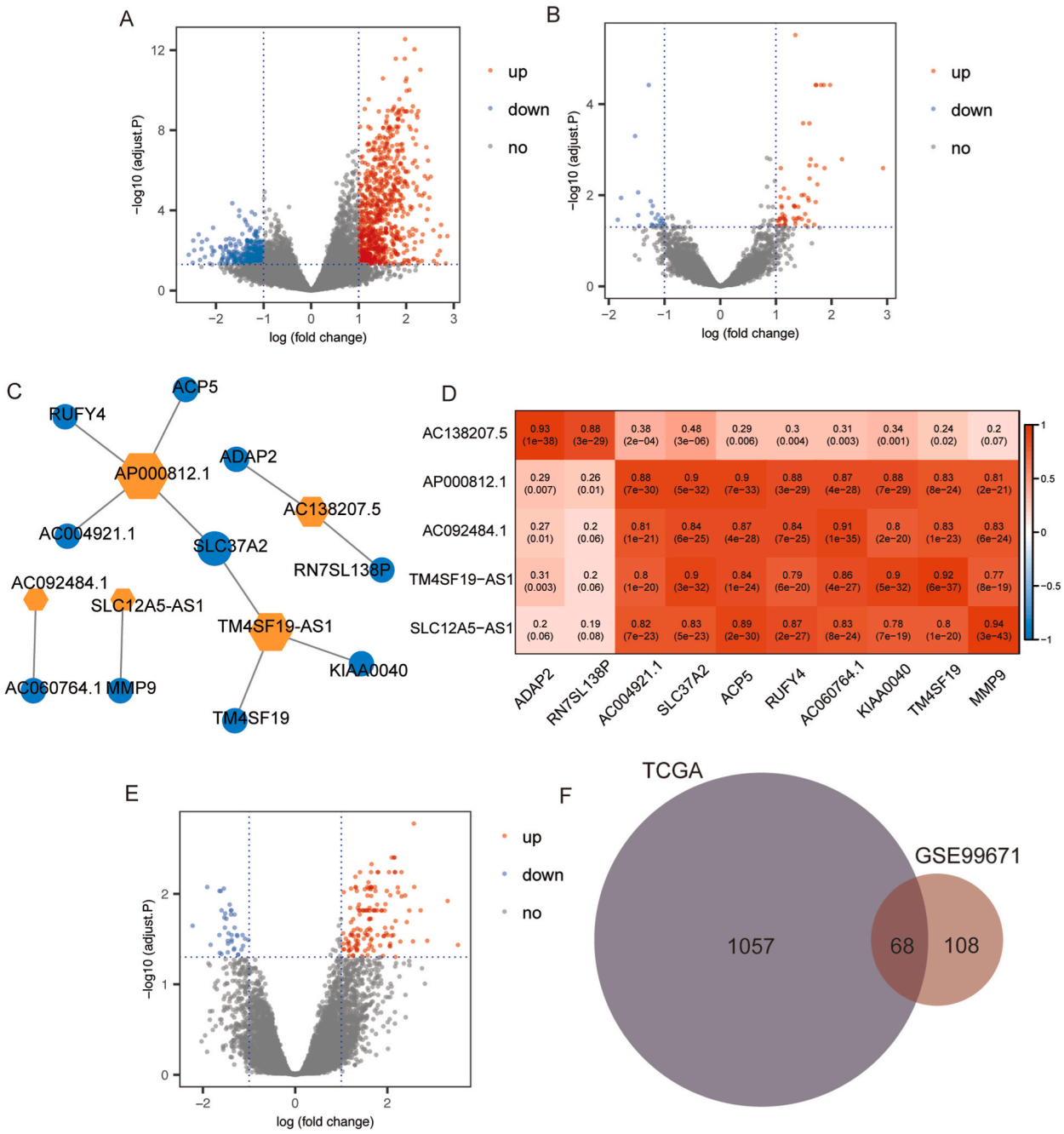

Fig. 3. Immune-related DEGs/DElncRNAs screening and lncRNA-mRNA co-expression analysis. Volcanic maps of DEGs (A) and DElncRNAs (B) in TCGA dataset; C: Co-expression analysis network diagram of DEGs and DElncRNAs; the yellow hexagon represents lncRNAs, and the blue circle represents mRNAs; D: Correlation matrix between co-expressed lncRNAs and mRNAs; the colored square indicates the correlation coefficient; red represents positive correlation, blue represents negative correlation (the darker the color is, the larger the correlation coefficient band); correlation coefficient and *P* values are marked in the box; E: Volcano map of GEO data machine GSE99671 DEGs; F: Venn diagram of intersections of DEGs in TCGA and GEO datasets. (For interpretation of the references to color in this figure legend, the reader is referred to the Web version of this article.)

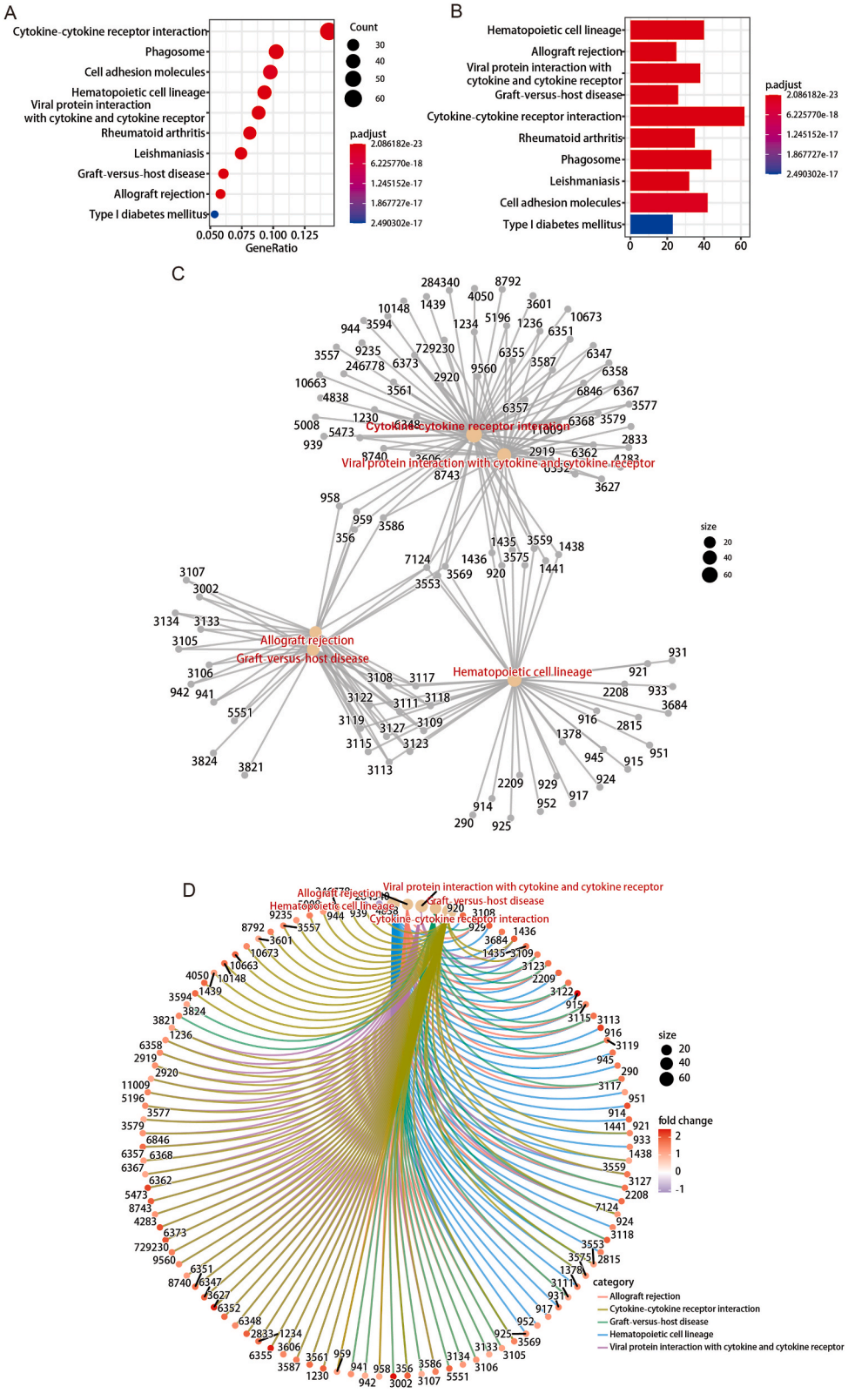

(caption on next page)

Fig. 4. KEGG analysis of immune-related DEGs. A: Bubble diagram of KEGG results; the closer the color is to red, the smaller *P* value is, and the larger the bubble is, the more DEGs are enriched in the pathway; B Bar graph of KEGG results; the closer the color is to red, the smaller the *P* value is, and the horizontal axis represents the number of genes enriched in the pathway; C: Network diagram of KEGG results; D: Cnetplot circle diagram of KEGG results. (For interpretation of the references to color in this figure legend, the reader is referred to the Web version of this article.)

multiple test corrections. For comparisons between two groups, the independent Student's *t*-test or Mann-Whitney *U* test was applied as appropriate. All statistical *P* values were obtained from bilateral tests, and $P < 0.05$ indicated statistical significance.

3. Results

3.1. Immune microenvironment assessment and immunization grouping

We used the ESTIMATE algorithm to calculate the immune invasion score of osteosarcoma patients in TCGA database, with a median score of 121.9 and a quartile range of 80.9–160.9, and compared the differences in immune invasion scores across clinical subgroups. No difference was observed in immune infiltrations among the groups with different ages, sex, and degrees (Fig. 1A–C), whereas significant differences were observed in the death/survival groups (Fig. 1D). The cutoff value of the score calculated using the *Maxstat* package was 125.3. Patients were divided into high and low immune infiltration groups based on the cutoff value, and a survival curve was generated. The results showed a difference in survival time between the groups (Fig. 1E).

CIBERSORT was employed to examine the infiltration of different immune cells. The infiltration of 22 types of immune cells is shown in Fig. 2A, among which M1 macrophages, M2 macrophages, and monocytes showed greater infiltration in the high immune score group. However, the degree of infiltration of resting dendritic cells, resting NK cells, naïve CD4 T cells, and gamma delta T cells was relatively higher in the group with low immunity scores. We analyzed the correlation between immune cells with significant differences in the degree of infiltration between the two groups; the correlation matrix is shown in Fig. 2B. The correlation between resting NK cells and naïve CD4 T cells was positive, and the absolute value of the coefficient was large. The correlation between M1 macrophages and naïve CD4 T cells was negative, and the absolute value of the coefficient was large.

3.2. Differentially expressed mRNA/lncRNA analysis and mRNA-lncRNA co-expression analysis

According to high/low immune infiltration grouping, 80 DElncRNAs were screened from TCGA lncRNA expression matrix using *limma* package, of which 57 were upregulated and 23 were downregulated. A total of 1125 DEGs were screened from TCGA mRNA expression matrix, of which 775 were upregulated and 350 were downregulated. The volcanic diagrams of the DElncRNAs and DEGs in TCGA dataset are shown in Fig. 3A–B. In the GEO dataset, differential expression analysis was also conducted according to the high/low grouping of immune infiltration (the median immunity score was used as a cutoff value), and 176 DEGs were identified, among which 68 were the same as those identified in TCGA dataset (Fig. 3E–F).

Co-expression analysis of 1125 immune-related DEGs and 80 DElncRNAs obtained from TCGA was performed. The PCC test was used to verify the relationship between mRNA and lncRNA levels (log2 transformation) in the pairs. Finally, a total of 11 pairs of lncRNA-mRNA were selected with an absolute value of PCC >0.9 and $P < 0.05$. The correlation results are presented in the form of a network (Fig. 3C), and the correlation matrix of the 11 lncRNA-mRNA pairs is shown in Fig. 3D.

3.3. Functional enrichment analysis of immune-related DEGs

KEGG analysis showed that the DEGs enrichment pathways mainly included hematopoietic cell lineage, allograft rejection, viral protein interaction with cytokines and cytokine receptors, graft-versus-host disease, and cytokine-cytokine receptor interaction (Fig. 4Ã D). GO analysis showed that DEGs were primarily related to T-cell activation, positive regulation of cell activation, positive adjustment of leukocyte activation, regulation of immune effector processes, leukocyte cell-cell adhesion, and other biological processes associated with cell components, such as immune receptor activity, antigen binding, cytokine activity, peptide antigen binding, and MHC protein complex binding, and associated with molecular function, such as the external side of the plasma membrane, tertiary granule, MHC protein complex, secretory granule membrane, and endocytic vesicle membrane (Fig. 5A&B). The pathways enriched by GSEA mainly involved the chemokine signaling pathway, hematopoietic cell lineage, Leishmania infection, cytokine receptor interaction, T-cell receptor signaling pathway, natural killer cell-mediated cytotoxicity, systemic lupus erythematosus, and cell adhesion molecule cascades (Fig. 6A–H). The GSVA results are presented in Fig. 6I–J. The DEGs enrichment pathways of the two datasets mainly included pathogenic Escherichia coli infection, vasopressin-regulated water reabsorption, adherens junctions, neurotrophin signaling pathways, and amyotrophic lateral sclerosis.

3.4. WGCNA

WGCNA was performed on the selected DElncRNAs (Fig. 7Ã E), and three modules that showed an association with immune cell infiltration were identified. Among these, module brown contained 30 genes, module blue contained 27 genes, and module turquoise contained 21 genes.

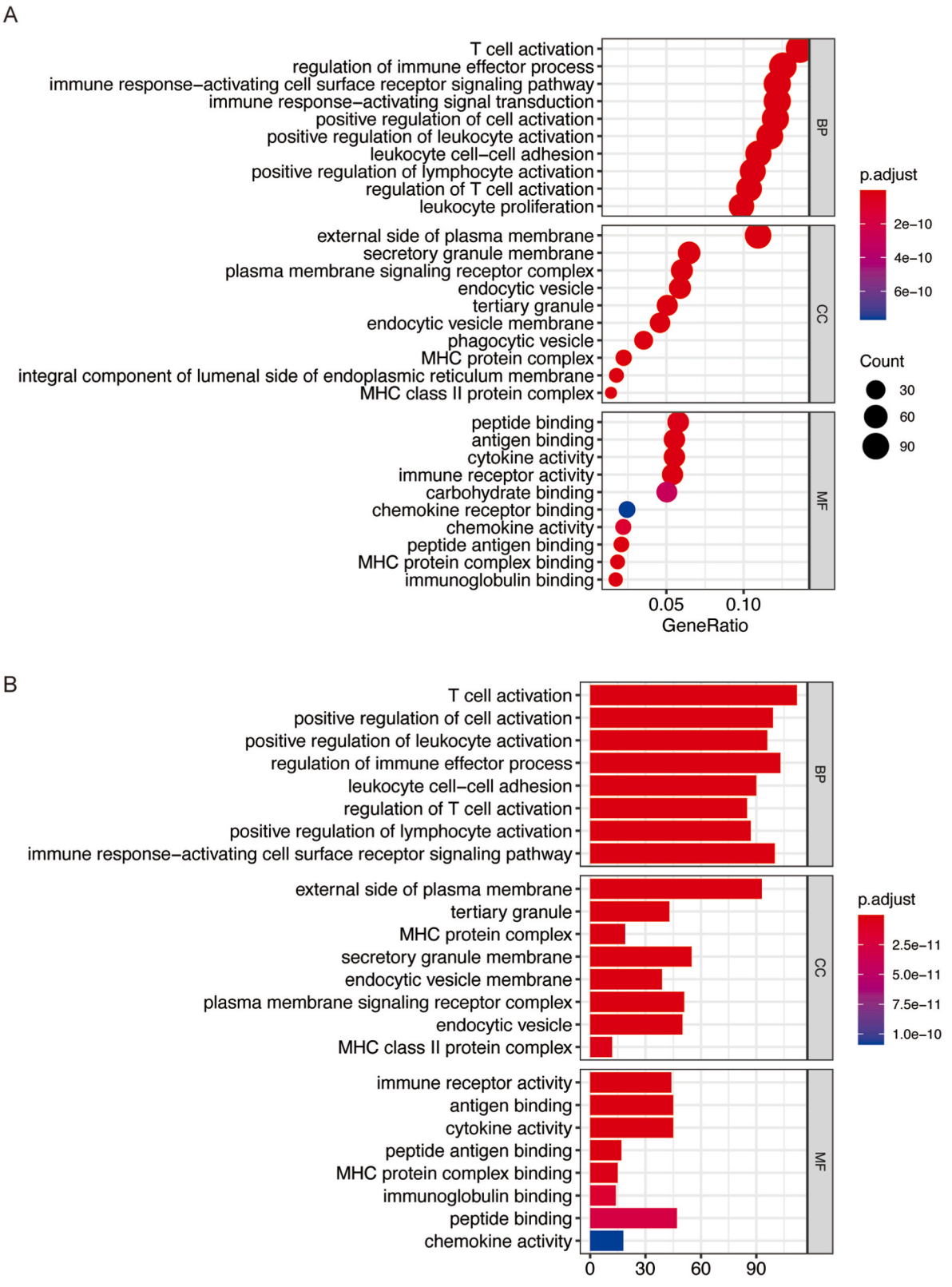

Fig. 5. GO enrichment analysis of immune-related DEGs. A: The enrichment results of biological process, cellular component, and molecular function analyzed by GO were presented in the form of a bubble graph; B: The enrichment results of biological process, cellular component, and molecular function in GO analysis were presented in a bar graph.

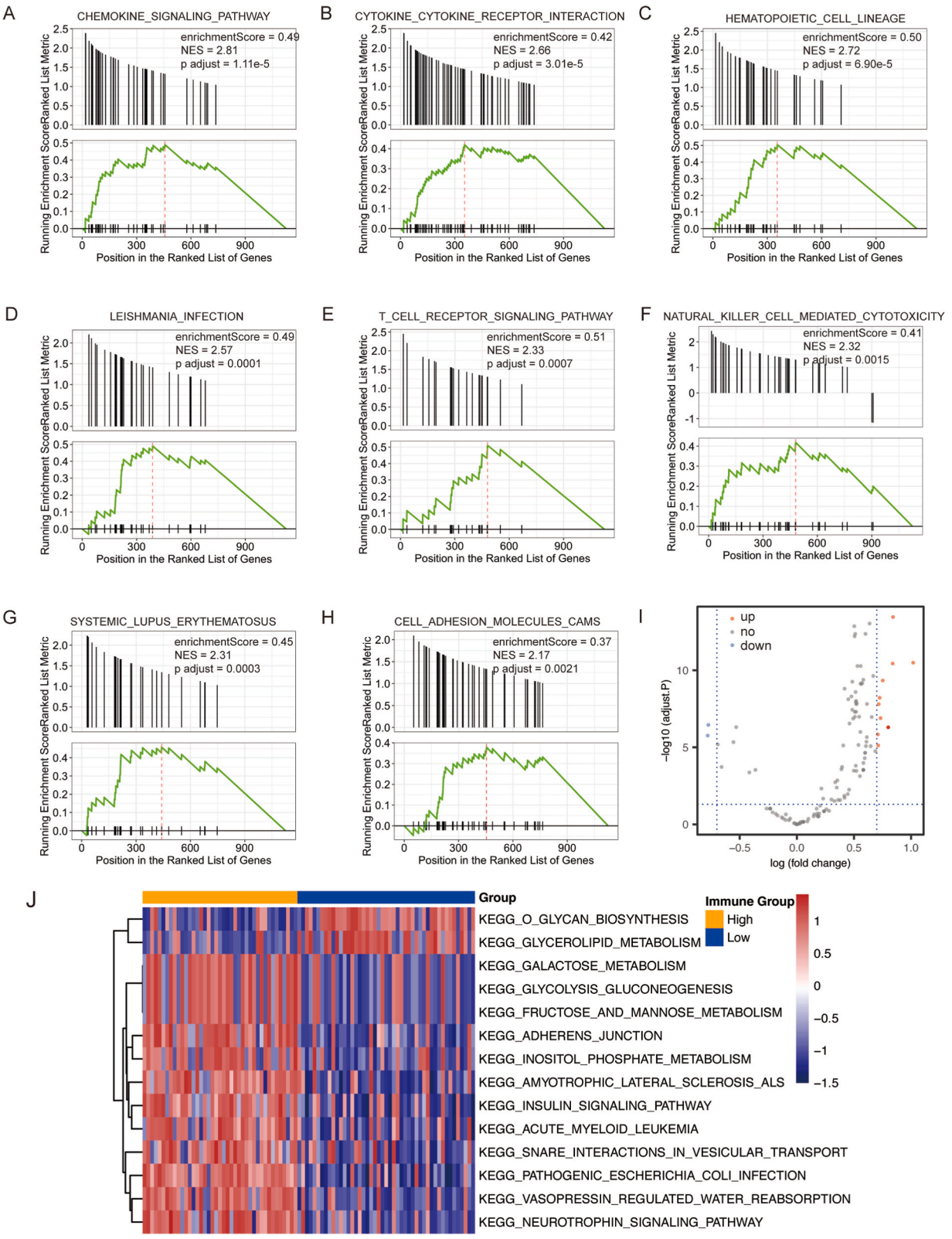

Fig. 6. GSEA and GSVA analysis of immune-associated DEGs. A–H: GSEA of enrichment pathways of immune-related DEGs; *P* value was determined by Kolmogorov–Smirnov test; I–J: the different pathways of immune-associated DEGs in GSVA analysis are shown in the volcanic map (I) and heat map (J).

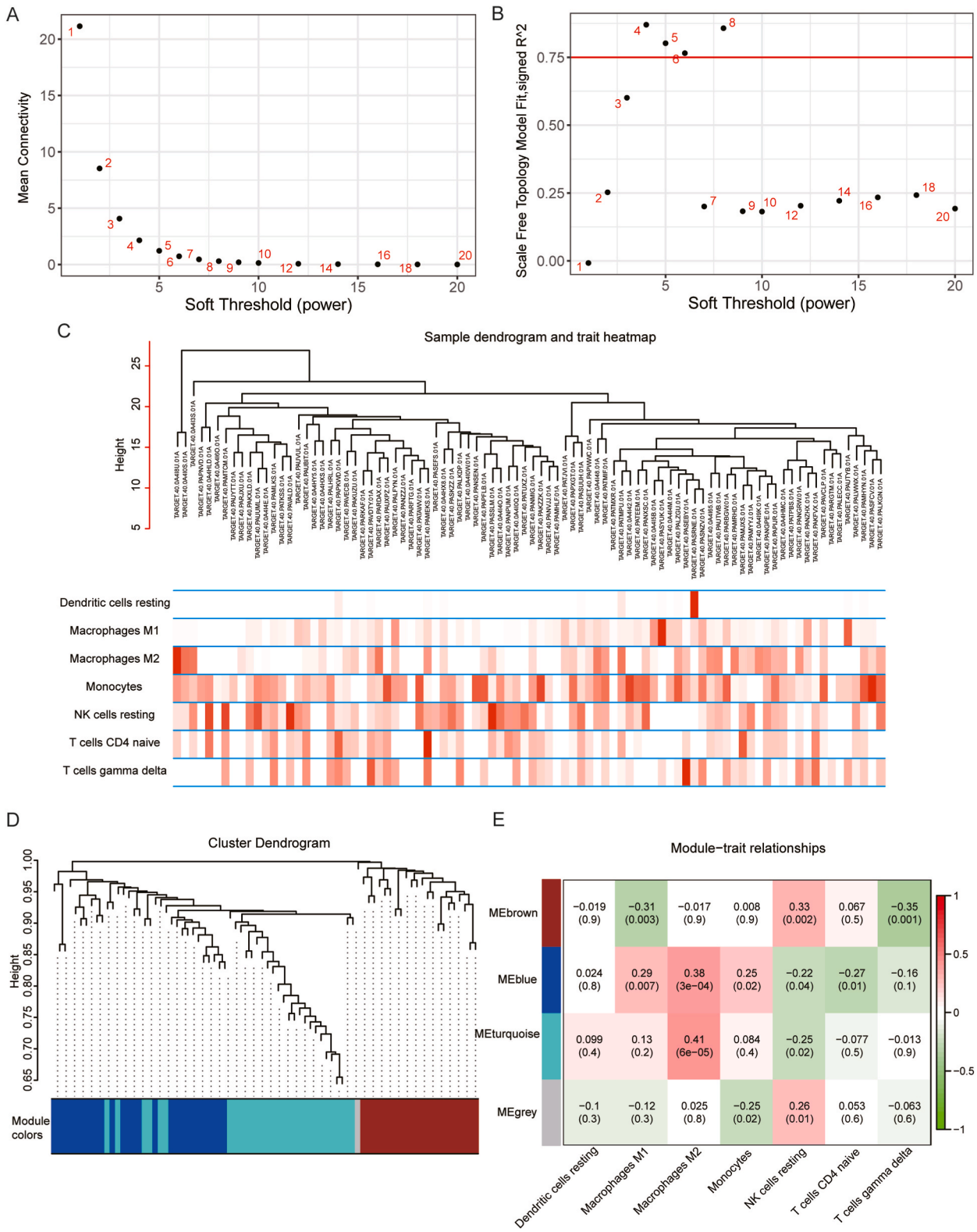

Fig. 7. WGCNA. A–B: Power parameter screening process; C: Cluster analysis tree diagram of samples and corresponding immune cell infiltration; D: Gene cluster analysis tree diagram; E: The correlation matrix between the module score and the degree of differential immune cell infiltration.

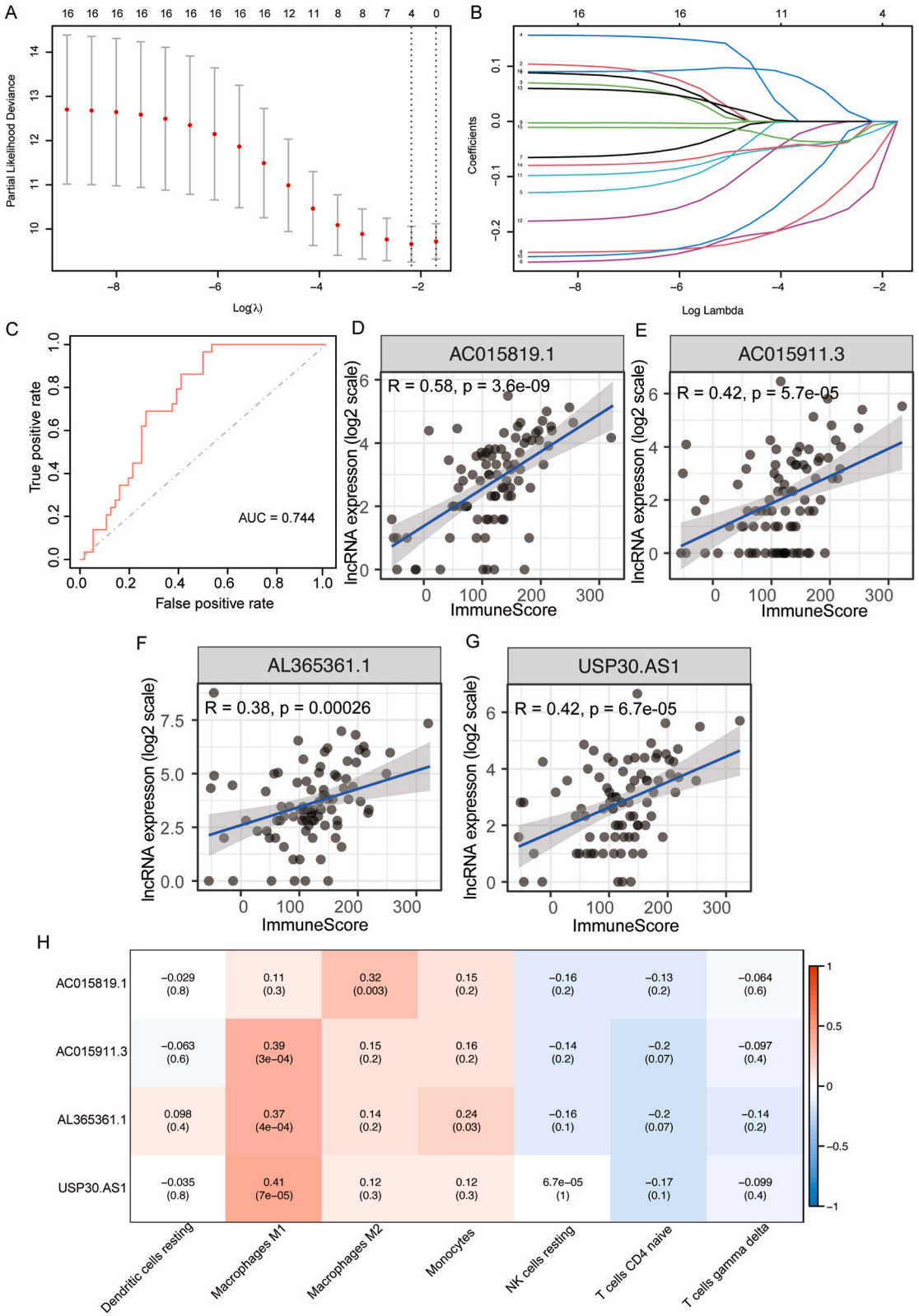

Fig. 8. Screening of prognostic lncRNAs by LASSO regression model. A–B: LASSO logistic regression model was used to screen prognostic markers; C: ROC curves; D–G: Correlation analysis of candidate prognostic lncRNAs and immune infiltration score; H: Correlation matrix between significantly different immune cells and candidate prognostic lncRNAs.

3.5. Prognostic marker screening

Univariate COX regression was used to identify the correlation between DElncRNAs and patient prognosis and survival of patients, and obtained 16 lncRNAs associated with prognosis were identified. Subsequently, LASSO regression analysis was performed and four lncRNAs were identified as prognostic markers (Fig. 8A–B), namely AC015819.1, AC015911.3, AL365361.1, and USP30.AS1. Details of these lncRNAs are listed in Table 1. The predictive ROC curve of LASSO regression showed an AUC value of 0.744, indicating a good prognostic ability (Fig. 8C). We then conducted a correlation analysis of the expression of these four lncRNAs and the immune infiltration score, which revealed a significant positive correlation between the candidate lncRNAs and the immune score (Fig. 8D–H). Finally, we evaluated their association with different immune cells and found that AC015911.3, AL365361.1, and USP30.AS1 were significantly and positively correlated with M1 macrophages.

3.6. RS and prognostic prediction model construction

According to the LASSO regression model, the coefficients of the candidate prognostic markers were determined, and the RS was calculated. The formula was as follows: RS = (−0.1203) * AC015819.1 + (−0.0644) * AC015911.3 + (−0.0186) * AL365361.1 + (−0.0067) * USP30.AS1. Subsequently, the Max*stat* package determined that the best cutoff for predicting the survival time of patients with osteosarcoma by RS was −0.6760. According to the cutoff value, patients with osteosarcoma were allocated to high/low-risk groups, and those without survival information were excluded. Finally, 29 and 56 patients were included in the low-and high-risk groups, respectively. The prognostic survival of patients with a high RS was lower than that of patients with a low RS (Fig. 9A). The ROC curves of 1-, 3-, and 5-year survival predicted by the RS are shown in Fig. 9B, among which the predictive ability for 5-year survival was the best (AUC = 0.769). Univariate Cox regression analysis showed that tumor metastasis had an impact on patient survival in addition to RS/grouping (Fig. 9C).

Based on tumor metastasis and RS, a COX regression model was applied to the multivariate prognostic prediction model. The forest plot is shown in Fig. 9D. The *rms* package was used to create a nomogram and calibration curve to predict the probability of survival at 1, 3, and 5 years in patients (Fig. 10Ã D). These variables were good predictors, as shown by the nomogram constructed using tumor metastasis (C-index = 0.701) or RS (C-index = 0.698) alone. The c-index of the survival prediction model constructed using the combination of metastasis and RS was 0.800, indicating better prognostic prediction ability.

3.7. AC015911.3 and AL365361.1 promote osteosarcoma

We first detected the expression of four lncRNAs in different osteosarcoma cells, and found that AC015911.3 and AL365361.1, had the highest expression in 143 B cells (Fig. 11A and B, Fig. S1A). There is no doubt that the content of TNF-α, one of the markers of the immune response, in 143B cells was significantly higher than that in hFOB 1.19 cells (Fig. 11C, Fig. S1B). We then focused on the molecular mechanisms of AC015911.3 and AL365361.1 in osteosarcoma. siRNA with three different sequences of AC015911.3 and AL365361.1, significantly reduced their expression in 143 B cells; among them, siAC015911.3–2 (siAC015911.3) and siAL365361.1–3 (siAL365361.1) had the most obvious effect (Fig. 11D and E). After knockdown of AC015911.3 and AL365361.1, cell viability decreased significantly in hFOB 1.19 cells (Fig. 11F) and 143 B cells (Fig. 11G). Similarly, after the knockdown of AC015911.3 and AL365361.1, cell invasion ability decreased (Fig. 11H) and apoptosis increased (Fig. 11I).

4. Discussion

Despite improvements in treatment strategies, most patients with metastatic or recurrent osteosarcoma have a poor prognosis [45]. Immunoreconstitution can inhibit osteosarcoma recurrence and improve the survival rate of metastatic osteosarcoma [46]. A previous study showed that abnormal lncRNA expression in osteosarcoma is highly linked to poor prognosis [47]. lncRNAs are conducive to the early diagnosis of osteosarcoma and contribute to improving the survival probability of patients with osteosarcoma [48]. Our study illustrates that lncRNAs (AC015819.1, AC015911.3, AL365361.1, and USP30.AS1) are potential prognostic biomarkers of osteosarcoma.

We downloaded the transcriptome data (mRNA + lncRNA) of patients with osteosarcoma (N = 88) from TCGA database. The transcriptome dataset GSE99671 (mRNA) for osteosarcoma (N = 18) and normal bone tissue (N = 18) was downloaded from the GEO database. The TIME is typically associated with immune cell invasion [49]. As expected, differences in immune infiltration scores were found in the TIME of patients with a death/survival outcome, suggesting that the TIME plays a role in the outcome of patients with osteosarcoma. Additionally, we found that the higher the degree of immune infiltration, the longer the survival time. In line with our

Table 1
Details of four lncRNAs annotated in LNCipedia.

lncRNA	Ensembl Gene ID	LNCipedia gene ID	Location (hg38)	Strand	Class	Transcript size
AC015819.1	ENSG00000273669	lnc-ZNF407-2	chr18:75073543–75074205	+	intergenic	663 bp
AC015911.3	ENSG00000267074	lnc-SLFN14-3	chr17:35499690–35510270	–	intronic	849 bp
AL365361.1	ENSG00000259834	lnc-KCNA3-3	chr1:110653560-110657040	–	intergenic	3481 bp
USP30-AS1	ENSG00000256262	USP30-AS1	chr12:109051791–109053971	–	antisense	1234 bp

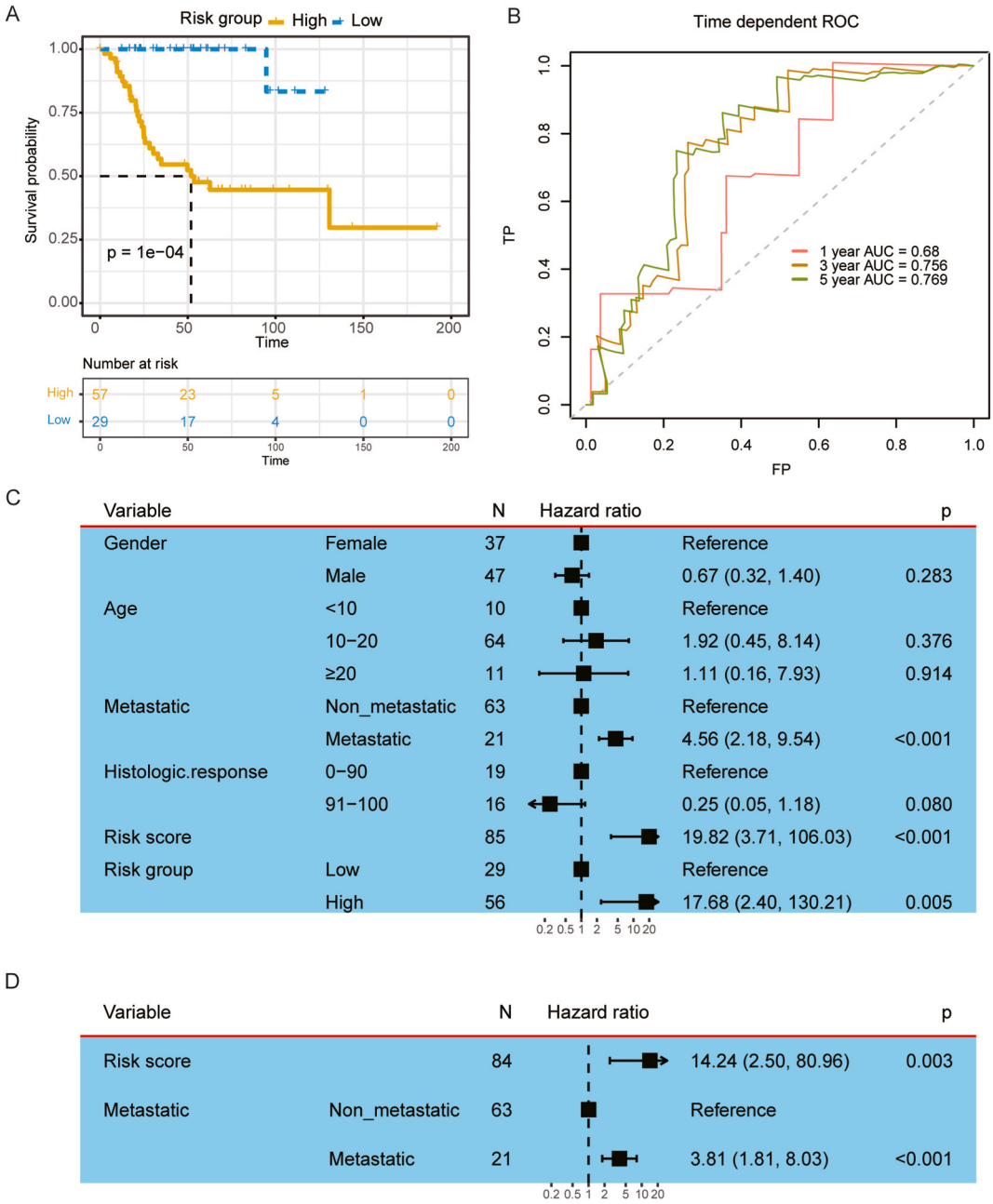

Fig. 9. Univariate and multivariate Cox regression analysis of RS for predicting clinical prognosis and survival in patients with osteosarcoma. A: Survival curves of the high/low RS groups; B: ROC curve; C: Univariate Cox regression analysis; D: Multivariate Cox regression analysis.

conclusion, the immune score of patients with osteosarcoma was associated with their survival outcomes, and a high immune score indicated that patients had an advantage in survival time [50]. Patients with osteosarcoma and reduced immune cell infiltration frequently have high metastasis rates and poor clinical outcomes [51]. Immune cells in the TIME are associated with tumor treatment and prognosis [15]. The TIME of osteosarcoma consists primarily of macrophages, T lymphocytes, and other subsets, such as B lymphocytes and mast cells [52]. The CIBERSORT algorithm further determined the proportion of infiltrating immune cells in the TIME of osteosarcoma. In our study, macrophages (M1, M2) and monocytes infiltrated more in the TIME of patients with a high immune score, whereas dendritic cells, resting NK cells, naïve CD4 T cells, and gamma delta T cells infiltrated patients with a low immune score. The proportions of memory B cells, naïve T cells, M2 macrophages, and activated NK cells are enhanced in high/low immune subsets [53]. Gomez-Brouchet et al. showed that the higher the tumor-associated macrophage infiltration, the lower the metastasis and the better the prognosis [54]. Hence, different immune cell infiltrates in osteosarcoma may serve as prognostic

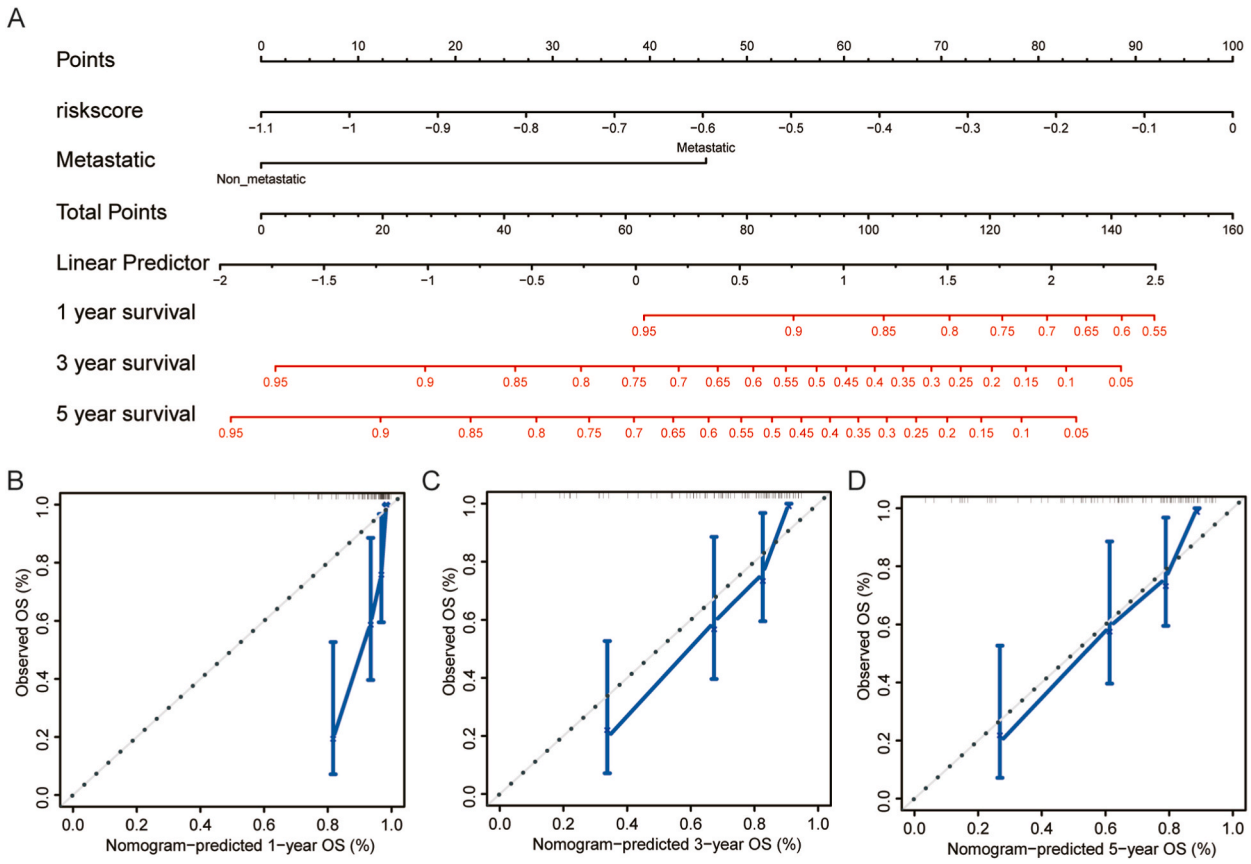

Fig. 10. Multivariate Cox regression model analysis of RS. A: Nomogram; and B–D: calibration curves.

indicators and immunotherapy targets.

Some lncRNAs are important regulators of TIME [55,56]. Abnormal expression is highly correlated with the occurrence and metastasis of tumors [57,58]. Several studies have shown the significant role of immune-related lncRNAs in the assessment of cancer patient prognosis [59,60]. A total of 80 DElncRNAs and 1125 DEGs were screened from TCGA database. To analyze their biological functions and explain their role in osteosarcoma, we subsequently conducted a co-expression analysis of DEGs and DElncRNAs and screened 11 lncRNA-mRNA pairs. Similarly, Shi et al. identified that lncRNA-C3orf35 and HMGB1 were linked to poor prognosis in osteosarcoma patients, and high levels of lncRNA-C3orf35 and HMGB1 were correlated with a low proportion of macrophage infiltration and low immune scores [61]. Next, we performed immune-related DEGs functional enrichment analysis to determine the functional categories and biological pathways of the DEGs. KEGG, GO, GSEA, and GSVA analyses revealed that the DEGs were involved in chemokine signaling pathways and cytokine-cytokine receptor interactions. Functional enrichment analysis revealed that immune responses and T-cell receptor cascades represented the main functions of immune-related genes in DEG between the high- and low-risk groups [62]. These deregulated immune genes may be the basis of TIME changes, and these findings provide a direction for further studies on immune response mechanisms.

WGCNA can identify a set of co-expressed genes (modules), and the modules can be associated with phenotypic data for analysis to mine potential marker genes [63]. Next, we performed WGCNA on the selected DElncRNAs and identified three modules that correlated with immune cell infiltration. Several studies have shown that lncRNAs are essential for predicting the prognosis of individuals [59,60]. To evaluate the association between DElncRNAs and the prognosis and survival of patients with osteosarcoma, the identified DElncRNAs were analyzed using univariate COX regression and LASSO regression. Four lncRNAs (AC015819.1, AC015911.3, AL365361.1, and USP30-AS1) were identified as prognostic markers (AUC = 0.744). Moreover, these four lncRNAs were positively correlated with immune infiltration scores. Most importantly, we found a significant positive correlation between M1 macrophages and AC015911.3, AL365361.1, and USP30.AS1. These genes are regulated by USP30.AS1 is mainly related in genetic regulation and the immune system [64]. The level of the immunophenotype-related lncRNA biomarker USP30-AS1 is correlated with immune cell infiltration in glioblastoma multiforme [65]. Five immune-related lncRNA signatures, including USP30-AS1, could predict the prognosis of cutaneous melanoma and contribute to immunotherapy [66]. Based on bioinformatics analyses, Zhang et al. revealed that certain lncRNAs (e.g., AL365361.1) with strong correlations with immune scores may modify the TIME of patients with high immune scores [67]. Taken together, the expression patterns of four lncRNAs (AC015819.1, AC015911.3, AL365361.1, and USP30-AS1) were associated with immune cell infiltration in osteosarcoma. The results of our experiments verified this hypothesis.

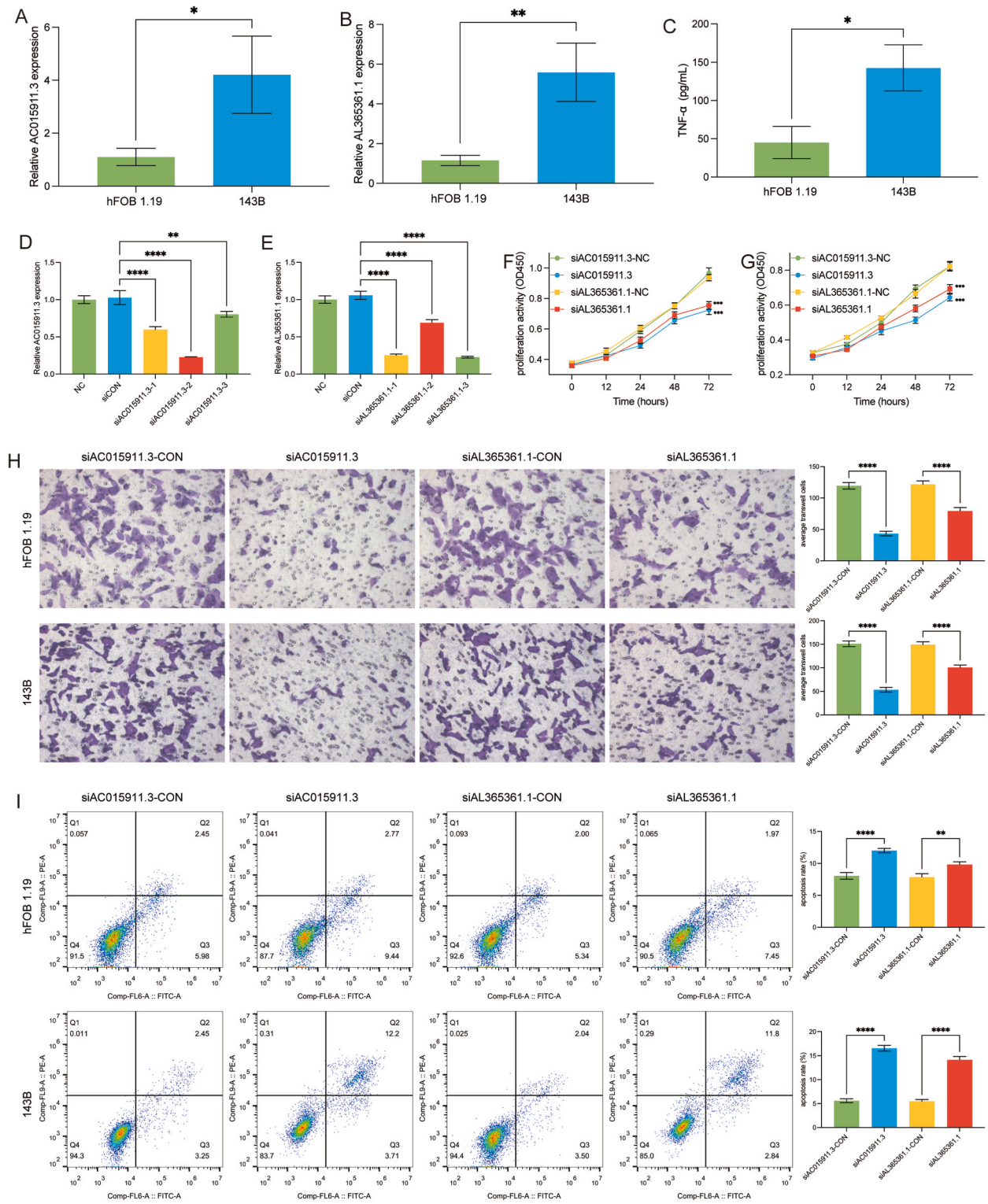

Fig. 11. AC015911.3 and AL365361.1 promote osteosarcoma. A: AC015911.3 was upregulated in the 143B cells; B: AL365361.1 was upregulated in the 143B cells; C: TNF-α was upregulated in the 143B cells; D: Verification of knockdown efficiency of AC015911.3; E: Verification of knockdown efficiency of AC015911.3; F: Knockdown of AC015911.3 and AL365361.1 decreased hFOB 1.19 cell viability; G: Knockdown of AC015911.3 and AL365361.1 decreased 143B cell viability; H: Knockdown of AC015911.3 and AL365361.1 decreased cell invasion ability; I: Knockdown of AC015911.3 and AL365361.1 increased cell apoptosis.

Metastasis and RS are two independent prognostic factors associated with overall survival in osteosarcoma patients [68]. Prior research has built an RS model to examine the prognosis of patients with osteosarcoma and lung adenocarcinoma based on tumor-infiltrating immune cells, and its prognostic value is superior to that of the TNM staging system. The immune RS model can be used to evaluate patients with recurrence risk [69,70]. The TNM staging system can be applied to stage-adapted therapy and prognostic prediction, showing more clinically relevant differentiation than the modified Masaoka staging system [71]. RS significantly correlated with metastasis, and high-risk patients were more likely to have tumor metastasis. A relevant study using Cox regression analysis illustrated that metastasis and RS were independent prognostic factors for osteosarcoma [72]. Furthermore, we constructed RS-and/or metastasis-dependent survival prediction models to assess patient outcomes. Interestingly, the results revealed that the two variables of tumor metastasis and RS alone could be used as good prognostic indicators, and the combination of the two variables showed better prognostic ability. The prognosis of patients at a high risk of osteosarcoma is worse than that of patients at a low risk, and tumor metastasis is another factor that affects the prognosis of patients [50,68]. Overall, the survival prediction model combined with metastasis and RS showed potential application for clinical prediction of the prognosis of patients with osteosarcoma.

However, this study has some limitations. First, the risk-scoring model was not validated in multicenter clinical trials or prospective studies. Second, the functions and mechanisms of these four immune-related lncRNAs remain unclear. Therefore, in future studies, we need to validate the risk-scoring model in multicenter clinical trials and prospective studies. Additionally, the functions and mechanisms of these four immune-related lncRNAs require further study.

5. Conclusions

Here, we identified abnormally regulated lncRNAs in osteosarcoma and lncRNAs (AC015819.1, AC015911.3, AL365361.1, and USP30.AS1) as potential biomarkers for OS prognosis.

Data availability statement

The authors confirm that the data supporting the findings of this study are available within the article.

Funding

This work was sponsored by Henan Provincial Medical Science and Technology Research Project [grant number LHGJ20220203].

CRediT authorship contribution statement

Bangmin Wang: Writing – original draft, Software, Formal analysis, Conceptualization. **Xin Wang:** Writing – original draft, Software, Methodology, Data curation. **Xinhui Du:** Writing – original draft, Visualization, Validation, Resources. **Shilei Gao:** Writing – original draft, Resources, Methodology, Investigation. **Bo Liang:** Writing – review & editing, Methodology, Formal analysis, Conceptualization. **Weitao Yao:** Writing – review & editing, Supervision, Methodology.

Declaration of competing interest

The authors declare that they have no known competing financial interests or personal relationships that could have appeared to influence the work reported in this paper.

Acknowledgments

We would like to thank all of the patients, investigators, and staff involved in the TARGET and GSE99671 studies who released and shared their data.

Appendix A. Supplementary data

Supplementary data to this article can be found online at https://doi.org/10.1016/j.heliyon.2024.e27023.

References

[1] N. Gaspar, Q. Campbell-Hewson, S. Gallego Melcon, et al., Phase I/II study of single-agent lenvatinib in children and adolescents with refractory or relapsed solid malignancies and young adults with osteosarcoma (ITCC-050)( ), ESMO Open 6 (5) (2021 Oct) 100250.
[2] L. Mirabello, R.J. Troisi, S.A. Savage, Osteosarcoma incidence and survival rates from 1973 to 2004: data from the Surveillance, Epidemiology, and End results Program, Cancer 115 (7) (2009 Apr 1) 1531–1543.
[3] M.J. Klein, G.P. Siegal, Osteosarcoma: anatomic and histologic variants, Am. J. Clin. Pathol. 125 (4) (2006 Apr) 555–581.
[4] G.N. Yan, Y.F. Lv, Q.N. Guo, Advances in osteosarcoma stem cell research and opportunities for novel therapeutic targets, Cancer Lett. 370 (2) (2016 Jan 28) 268–274.

[5] Y. Yu, H. Zhang, T. Ren, et al., Development of a prognostic gene signature based on an immunogenomic infiltration analysis of osteosarcoma, J. Cell Mol. Med. 24 (19) (2020 Oct) 11230–11242.
[6] S. Bagcchi, Osteosarcoma survivors' risk of second cancer, Lancet Oncol. 15 (10) (2014 Sep) e425.
[7] K. Hayakawa, S. Matsumoto, K. Ae, et al., Definitive surgery of primary lesion should be prioritized over preoperative chemotherapy to treat high-grade osteosarcoma in patients aged 41-65 years, J. Orthop. Traumatol. 21 (1) (2020 Aug 31) 13.
[8] C. Meazza, S.D. Asaftei, State-of-the-art, approved therapeutics for the pharmacological management of osteosarcoma, Expert Opin Pharmacother 22 (15) (2021 Oct) 1995–2006.
[9] J.A. Park, N.V. Cheung, GD2 or HER2 targeting T cell engaging bispecific antibodies to treat osteosarcoma, J. Hematol. Oncol. 13 (1) (2020 Dec 10) 172.
[10] D. Hanahan, L.M. Coussens, Accessories to the crime: functions of cells recruited to the tumor microenvironment, Cancer Cell 21 (3) (2012 Mar 20) 309–322.
[11] D.W. Edwardson, A.M. Parissenti, A.T. Kovala, Chemotherapy and inflammatory cytokine signalling in cancer cells and the tumour microenvironment, Adv. Exp. Med. Biol. 1152 (2019) 173–215.
[12] C. Hu, C. Liu, S. Tian, et al., Comprehensive analysis of prognostic tumor microenvironment-related genes in osteosarcoma patients, BMC Cancer 20 (1) (2020 Aug 27) 814.
[13] C. Zhang, J.H. Zheng, Z.H. Lin, et al., Profiles of immune cell infiltration and immune-related genes in the tumor microenvironment of osteosarcoma, Aging (Albany NY) 12 (4) (2020 Feb 9) 3486–3501.
[14] P. Koirala, M.E. Roth, J. Gill, et al., Immune infiltration and PD-L1 expression in the tumor microenvironment are prognostic in osteosarcoma, Sci. Rep. 6 (2016 Jul 26) 30093.
[15] Q. Huang, Y. Lin, C. Chen, et al., Immune-related LncRNAs affect the prognosis of osteosarcoma, which are related to the tumor immune microenvironment, Front. Cell Dev. Biol. 9 (2021) 731311.
[16] Y.Y. Mi, C.Y. Sun, L.F. Zhang, et al., Long non-coding RNAs LINC01679 as a Competitive Endogenous RNAs inhibits the Development and progression of Prostate cancer via regulating the miR-3150a-3p/SLC17A9 Axis, Front. Cell Dev. Biol. 9 (2021) 737812.
[17] X. Meng, Z.F. Wang, Q.Y. Lou, et al., Long non-coding RNAs in head and neck squamous cell carcinoma: diagnostic biomarkers, targeted therapies, and prognostic roles, Eur. J. Pharmacol. 902 (2021 Jul 5) 174114.
[18] Y. Fang, M.J. Fullwood, Roles, functions, and mechanisms of long non-coding RNAs in cancer, Dev. Reprod. Biol. 14 (1) (2016 Feb) 42–54.
[19] J. Wei, D.L. Fang, C.K. Huang, et al., Screening a novel signature and predicting the immune landscape of metastatic osteosarcoma in children via immune-related lncRNAs, Transl. Pediatr. 10 (7) (2021 Jul) 1851–1866.
[20] S. Huang, C. Sun, Y. Hou, et al., Author Correction: a comprehensive bioinformatics analysis on multiple Gene Expression Omnibus datasets of nonalcoholic fatty liver disease and nonalcoholic steatohepatitis, Sci. Rep. 9 (1) (2019 May 3) 7105.
[21] C. Huang, Q. Wang, S. Ma, et al., A four serum-miRNA panel serves as a potential diagnostic biomarker of osteosarcoma, Int. J. Clin. Oncol. 24 (8) (2019 Aug) 976–982.
[22] Y. Liu, J. Guan, X. Chen, Identification of differentially expressed genes under the regulation of transcription factors in osteosarcoma, Pathol. Oncol. Res. 25 (3) (2019 Jul) 1091–1102.
[23] X.D. Ho, P. Phung, V. Ql, et al., Whole transcriptome analysis identifies differentially regulated networks between osteosarcoma and normal bone samples, Exp Biol Med (Maywood). 242 (18) (2017 Dec) 1802–1811.
[24] K. Yoshihara, M. Shahmoradgoli, E. Martinez, et al., Inferring tumour purity and stromal and immune cell admixture from expression data, Nat. Commun. 4 (2013) 2612.
[25] T. Hothorn, A. Zeileis, Generalized maximally selected statistics, Biometrics 64 (4) (2008 Dec) 1263–1269.
[26] A.M. Newman, C.L. Liu, M.R. Green, et al., Robust enumeration of cell subsets from tissue expression profiles, Nat. Methods 12 (5) (2015 May) 453–457.
[27] M.E. Ritchie, B. Phipson, D. Wu, et al., Limma powers differential expression analyses for RNA-sequencing and microarray studies, Nucleic Acids Res. 43 (7) (2015 Apr 20) e47.
[28] Y.J. Liu, S.Y. Yin, S.H. Zeng, et al., Prognostic value of LHFPL Tetraspan Subfamily member 6 (LHFPL6) in Gastric cancer: a study based on bioinformatics analysis and experimental validation, Pharmgenomics Pers Med 14 (2021) 1483–1504.
[29] D. Otasek, J.H. Morris, J. Boucas, et al., Cytoscape Automation: empowering workflow-based network analysis, Genome Biol. 20 (1) (2019 Sep 2) 185.
[30] M.A. Harris, J. Clark, A. Ireland, et al., The Gene Ontology (GO) database and informatics resource, Nucleic Acids Res. 32 (Database issue) (2004 Jan 1) D258–D261.
[31] M. Kanehisa, S. Goto, KEGG: kyoto encyclopedia of genes and genomes, Nucleic Acids Res. 28 (1) (2000 Jan 1) 27–30.
[32] G. Yu, L.G. Wang, Y. Han, et al., clusterProfiler: an R package for comparing biological themes among gene clusters, OMICS 16 (5) (2012 May) 284–287.
[33] S. Hanzelmann, R. Castelo, J. Guinney, GSVA: gene set variation analysis for microarray and RNA-seq data, BMC Bioinf. 14 (2013 Jan 16) 7.
[34] P. Langfelder, S. Horvath, WGCNA: an R package for weighted correlation network analysis, BMC Bioinf. 9 (2008 Dec 29) 559.
[35] P.-J. Volders, J. Anckaert, K. Verheggen, et al., LNCipedia 5: towards a reference set of human long non-coding RNAs, Nucleic Acids Res. 47 (D1) (2019 Jan 8) D135–D139.
[36] T. Sun, T. Wang, Y. Qiu, et al., A Sarcopenia-based prediction model for Postoperative Complications of ex vivo liver resection and Autotransplantation to treat End-stage Hepatic Alveolar Echinococcosis, Infect. Drug Resist. 14 (2021) 4887–4901.
[37] S. Engebretsen, J. Bohlin, Statistical predictions with glmnet, Clin Epigenetics 11 (1) (2019 Aug 23) 123.
[38] P.J. Heagerty, T. Lumley, M.S. Pepe, Time-dependent ROC curves for censored survival data and a diagnostic marker, Biometrics 56 (2) (2000 Jun) 337–344.
[39] W. Tu, E. Johnson, E. Fujiwara, et al., Predictive variables for peripheral neuropathy in treated HIV type 1 infection revealed by machine learning, AIDS 35 (11) (2021 Sep 1) 1785–1793.
[40] W.-C. Lu, H. Chen, B. Liang, et al., Integrative analyses and Verification of the expression and prognostic significance for RCN1 in glioblastoma multiforme [original research], Front. Mol. Biosci. 8 (2021 2021-October-13) 736947.
[41] B. Liang, X.-X. Zhang, R. Li, et al., Guanxin V protects against ventricular remodeling after acute myocardial infarction through the interaction of TGF-β1 and Vimentin, Phytomedicine 95 (2022) 153866, 2022/01/01/.
[42] B. Liang, X.-X. Zhang, R. Li, et al., Guanxin V alleviates acute myocardial infarction by restraining oxidative stress damage, apoptosis, and fibrosis through the TGF-β1 signalling pathway, Phytomedicine 100 (2022) 154077, 2022/03/27/.
[43] X.-X. Zhang, C.-L. Shao, S.-Y. Cheng, et al., Effect of Guanxin V in animal model of acute myocardial infarction, BMC Complement Med Ther 21 (1) (2021) 72.
[44] B. Liang, Y. Liang, R. Li, et al., Integrating systematic pharmacology-based strategy and experimental validation to explore the synergistic pharmacological mechanisms of Guanxin V in treating ventricular remodeling, Bioorg. Chem. 115 (2021) 105187, 2021/10/01/.
[45] Z. Li, P. Dou, T. Liu, et al., Application of long noncoding RNAs in osteosarcoma: biomarkers and therapeutic targets, Cell. Physiol. Biochem. 42 (4) (2017) 1407–1419.
[46] M.S. Merchant, D. Bernstein, M. Amoako, et al., Adjuvant immunotherapy to improve outcome in high-risk Pediatric sarcomas, Clin. Cancer Res. 22 (13) (2016 Jul 1) 3182–3191.
[47] Z. Yang, X. Li, Y. Yang, et al., Long noncoding RNAs in the progression, metastasis, and prognosis of osteosarcoma, Cell Death Dis. 7 (9) (2016 Sep 29) e2389.
[48] X. Bu, J. Liu, R. Ding, et al., Prognostic value of a Pyroptosis-related long noncoding RNA signature associated with osteosarcoma microenvironment, J Oncol 2021 (2021) 2182761.
[49] C. Kaltenmeier, H.O. Yazdani, K. Morder, et al., Neutrophil extracellular Traps promote T cell Exhaustion in the tumor microenvironment, Front. Immunol. 12 (2021) 785222.
[50] D. Zheng, K. Yang, X. Chen, et al., Analysis of immune-stromal score-based gene signature and molecular Subtypes in osteosarcoma: Implications for prognosis and tumor immune microenvironment, Front. Genet. 12 (2021) 699385.
[51] M.C. Scott, N.A. Temiz, A.E. Sarver, et al., Comparative transcriptome analysis Quantifies immune cell transcript levels, metastatic progression, and survival in osteosarcoma, Cancer Res. 78 (2) (2018 Jan 15) 326–337.

[52] M.F. Heymann, F. Lezot, D. Heymann, The contribution of immune infiltrates and the local microenvironment in the pathogenesis of osteosarcoma, Cell. Immunol. 343 (2019 Sep) 103711.
[53] Z. Chen, H. Kong, Z. Cai, et al., Identification of MAP3K15 as a potential prognostic biomarker and correlation with immune infiltrates in osteosarcoma, Ann. Transl. Med. 9 (14) (2021 Jul) 1179.
[54] A. Gomez-Brouchet, C. Illac, J. Gilhodes, et al., CD163-positive tumor-associated macrophages and CD8-positive cytotoxic lymphocytes are powerful diagnostic markers for the therapeutic stratification of osteosarcoma patients: an immunohistochemical analysis of the biopsies fromthe French OS2006 phase 3 trial, OncoImmunology 6 (9) (2017) e1331193.
[55] L. Ding, J. Ren, D. Zhang, et al., A novel stromal lncRNA signature reprograms fibroblasts to promote the growth of oral squamous cell carcinoma via LncRNA-CAF/interleukin-33, Carcinogenesis 39 (3) (2018 Mar 8) 397–406.
[56] Y. Luo, J. Yang, J. Yu, et al., Long non-coding RNAs: Emerging roles in the Immunosuppressive tumor microenvironment, Front. Oncol. 10 (2020) 48.
[57] N. Bartonicek, J.L. Maag, M.E. Dinger, Long noncoding RNAs in cancer: mechanisms of action and technological advancements, Mol. Cancer 15 (1) (2016 May 27) 43.
[58] J.W. Kornfeld, J.C. Bruning, Regulation of metabolism by long, non-coding RNAs, Front. Genet. 5 (2014) 57.
[59] Y. Li, T. Jiang, W. Zhou, et al., Pan-cancer characterization of immune-related lncRNAs identifies potential oncogenic biomarkers, Nat. Commun. 11 (1) (2020 Feb 21) 1000.
[60] Y. Shen, X. Peng, C. Shen, Identification and validation of immune-related lncRNA prognostic signature for breast cancer, Genomics 112 (3) (2020 May) 2640–2646.
[61] Y. Shi, J. Ren, Z. Zhuang, et al., Comprehensive analysis of a ceRNA network identifies lncR-C3orf35 associated with poor prognosis in osteosarcoma, BioMed Res. Int. 2020 (2020) 3178037.
[62] F.P. Zhang, Y.P. Huang, W.X. Luo, et al., Construction of a risk score prognosis model based on hepatocellular carcinoma microenvironment, World J. Gastroenterol. 26 (2) (2020 Jan 14) 134–153.
[63] Z. Chen, H. Huang, Y. Wang, et al., Identification of immune-related genes MSR1 and TLR7 in relation to macrophage and type-2 T-Helper cells in osteosarcoma tumor Micro-Environments as Anti-metastasis signatures, Front. Mol. Biosci. 7 (2020) 576298.
[64] W. Zhou, S. Xu, T. Deng, et al., LncRNA USP30-AS1 promotes the survival of acute myeloid leukemia cells by cis-regulating USP30 and ANKRD13A, Hum. Cell 35 (1) (2022 Jan) 360–378.
[65] M. Gao, X. Wang, D. Han, et al., A Six-lncRNA signature for immunophenotype prediction of glioblastoma multiforme, Front. Genet. 11 (2020) 604655.
[66] L. Xue, P. Wu, X. Zhao, et al., Using immune-related lncRNA signature for prognosis and response to immunotherapy in cutaneous melanoma, Int. J. Gen. Med. 14 (2021) 6463–6475.
[67] Z. Zhong, M. Hong, X. Chen, et al., Transcriptome analysis reveals the link between lncRNA-mRNA co-expression network and tumor immune microenvironment and overall survival in head and neck squamous cell carcinoma, BMC Med Genomics 13 (1) (2020 Mar 30) 57.
[68] J. Zhang, R. Ding, T. Wu, et al., Autophagy-related genes and long noncoding RNAs signatures as predictive biomarkers for osteosarcoma survival, Front. Cell Dev. Biol. 9 (2021) 705291.
[69] Y. Chen, B. Zhao, X. Wang, Tumor infiltrating immune cells (TIICs) as a biomarker for prognosis benefits in patients with osteosarcoma, BMC Cancer 20 (1) (2020 Oct 21) 1022.
[70] Y. Pan, Y. Sha, H. Wang, et al., Comprehensive analysis of the association between tumor-infiltrating immune cells and the prognosis of lung adenocarcinoma, J Cancer Res Ther 16 (2) (2020) 320–326.
[71] Y.C. Tseng, H.S. Hsu, Y.H. Lin, et al., Does Size Affect the Prognosis of Resectable Thymoma beyond the Eighth Edition TNM? Thorac Cancer, 2021 Dec 20.
[72] J. Zhang, X. Miao, T. Wu, et al., Development and validation of Ten-RNA binding protein signature predicts overall survival in osteosarcoma, Front. Mol. Biosci. 8 (2021) 751842.